The EMBO Journal vol.15 no.22 pp.6011–6017, 1996

The ornithodorin–thrombin crystal structure, a key to the TAP enigma?

Andreas van de Locht[1], Milton T.Stubbs, Wolfram Bode, Thomas Friedrich[2], Claus Bollschweiler[2], Wolfgang Höffken[2] and Robert Huber[1]

Max-Planck-Institut für Biochemie, Abteilung Strukturforschung, 82152 Martinsried and [2]Abteilung für Biotechnologie, BASF Aktiengesellschaft, 67056 Ludwigshafen, Germany

[1]Corresponding authors

Ornithodorin, isolated from the blood sucking soft tick *Ornithodoros moubata*, is a potent (K_i = 10^{-12} M) and highly selective thrombin inhibitor. Internal sequence homology indicates a two domain protein. Each domain resembles the Kunitz inhibitor basic pancreatic trypsin inhibitor (BPTI) and also the tick anticoagulant peptide (TAP) isolated from the same organism. The 3.1 Å crystal structure of the ornithodorin–thrombin complex confirms that both domains of ornithodorin exhibit a distorted BPTI-like fold. The N-terminal portion and the C-terminal helix of each domain are structurally very similar to BPTI, whereas the regions corresponding to the binding loop of BPTI adopt different conformations. Neither of the two 'reactive site loops' of ornithodorin contacts the protease in the ornithodorin–thrombin complex. Instead, the N-terminal residues of ornithodorin bind to the active site of thrombin, reminiscent of the thrombin–hirudin interaction. The C-terminal domain binds at the fibrinogen recognition exosite. Molecular recognition of its target protease by this double-headed Kunitz-type inhibitor diverges considerably from other members of this intensely studied superfamily. The complex structure provides a model to explain the perplexing results of mutagenesis studies on the TAP–factor Xa interaction.

Keywords: BPTI/coagulation/factor Xa/inhibitor/Kunitz module

Introduction

The serine proteinase α-thrombin (EC 3.4.21.5) is the key enzyme in haemostasis and thrombosis. Several unique structural features contribute to its enhanced specificity and selectivity towards macromolecular substrates and inhibitors (Bode *et al.*, 1992; Stubbs and Bode, 1993). Notably, characteristic insertion loops restrict access to the active site, such that typical serine proteinase inhibitors such as basic pancreatic trypsin inhibitor (BPTI) are unable to inhibit thrombin. Thrombin exhibits a distinctive charge distribution, with two basic exosites: the fibrinogen recognition exosite and the heparin binding site. The former plays a central function in selection of thrombin substrates and inhibitors, whilst the latter site is of importance for the heparin-modulated inhibition of thrombin by the serpins antithrombin III, heparin cofactor II and proteinase nexin I (reviewed in Stubbs and Bode, 1995).

More than 60 sequences of BPTI-like proteins are known, the Kunitz superfamily, spanning the animal kingdom from sea anemone to man. Members of this superfamily show highly conserved regions, an invariant cysteine spacing (reviewed in Laskowski and Kato, 1980) and virtually identical tertiary structure according to the seven atomic structures determined to date (Huber *et al.*, 1970; Lancelin *et al.*, 1994; Kwong *et al.*, 1995; see Antuch *et al.;* 1993). The BPTI–trypsin interaction serves as a paradigm for the 'canonical' inhibition of serine proteinases (Bode and Huber, 1992); according to the 'standard mechanism' (Laskowski and Kato, 1980) the inhibitor interacts with its cognate enzyme via a substrate-like binding loop involved in antiparallel β-sheet formation with residues in the vicinity of the active site. Although the inhibitory members of this superfamily are relatively widespread, no thrombin inhibitor has been found among them. The affinity of BPTI for human α-thrombin is $<10^{-4}$ M (Ascenzi *et al.*, 1988); docking studies of BPTI to the active site of thrombin suggested steric hindrance and collision of the inhibitor with the thrombin 60loop, most of all the very prominent Trp60D (Bode *et al.*, 1992). [The thrombin nomenclature used is that suggested by Bode *et al.*, 1989; ornithodorin residues are identified in the text by a prime; BPTI residues are distinguished by the suffix I; amino acids in TAP are designated by the suffix T or (T) for mutants.]

To prevent clotting of their victim's blood, haematophageous animals have developed a battery of anti-clotting mechanisms (for a review see Markwardt, 1994). Many of these animals contain a cocktail of several anticoagulants, among which the thrombin inhibitors are the most prominent. The complex of thrombin with the highly potent inhibitor hirudin from the medicinal leech *Hirudo medicinalis* revealed a distinctly non-canonical interaction (Grütter *et al.*, 1990; Rydel *et al.*, 1990). The hirudin globular N-terminal domain sits over the active site, with its N-terminal residues contacting the thrombin active site through parallel β-sheet formation. Simultaneously, the hirudin acidic C-terminal tail occupies the fibrinogen recognition exosite. The thrombin complex with rhodniin from the assassin bug *Rhodnius prolixus* provided the first example of a canonical inhibitor of thrombin (van de Locht *et al.*, 1995). Rhodniin consists of two modified Kazal-type domains, with the binding loop of the N-terminal domain bound like a substrate in the active site and the acidic C-terminal domain bound at the fibrinogen recognition exosite.

The soft tick *Ornithodoros moubata* is a particularly rich source of anticoagulatory activity; in addition to the thrombin inhibitor ornithodorin (M.Otte, A.van de Locht,

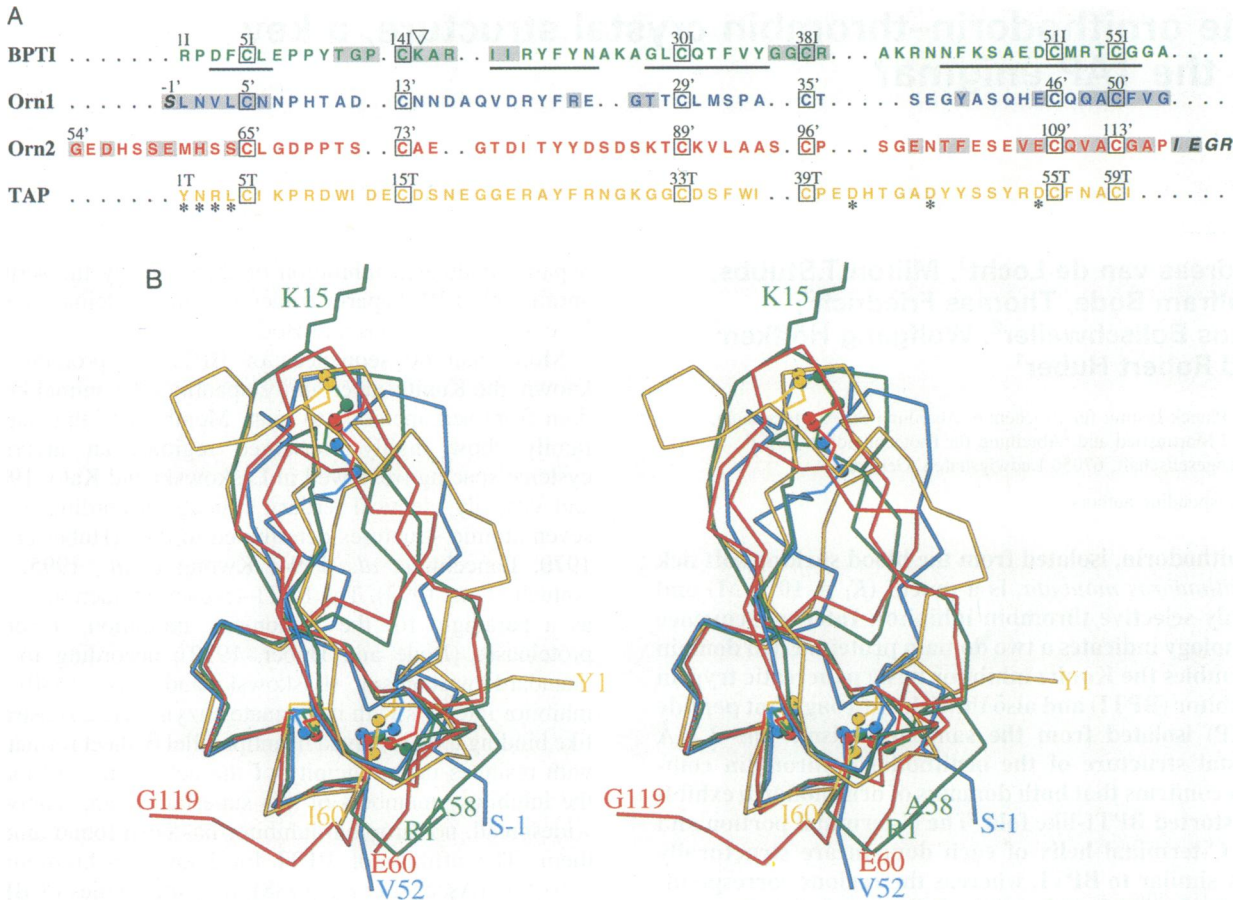

Fig. 1. Sequence information and superposition of the four Kunitz domains. (**A**) Structure-based sequence alignment of BPTI, the two domains of ornithodorin and TAP. Underlined regions indicate structurally similar parts which were used for the alignment. The cysteine residues are aligned to show insertions and deletions in the respective Kunitz-type domains. Shaded positions refer to residues that are involved in contacts with trypsin for BPTI (Huber *et al.*, 1974) and thrombin for ornithodorin respectively. The arrow denotes the P1 residue (Lys15I) of BPTI. Stars indicate residues of TAP that show >2-fold changes in K_i upon mutation (Dunwiddie *et al.*, 1992; Mao *et al.*, 1995). Bold italic letters denote residues deviating from the wild-type sequence that were introduced for recombinant expression. The aligned sequences were formatted using the program ALSCRIPT (Barton, 1993). (**B**) Superposition of BPTI (green), the N-terminal (cyan) and C-terminal (red) domains of ornithodorin and TAP (orange). The first and last residues of each domain are labelled in its respective colour. The P1 -residue of the BPTI binding loop is shown. Disulfide bridges are displayed as ball-and-stick. Figure prepared using MOLSCRIPT (Kraulis, 1991).

T.Friedrich, S.Bialojan, B.Kröger, C.Bollsch-Weiler, J.Dodt, E.A.Auerswald, W.Bode and H.Fritz, in preparation) and the factor Xa inhibitor tick anticoagulant peptide (TAP) (Waxman *et al.*, 1990; Vlasuk, 1993), an inhibitory activity against platelet aggregation (Waxman and Connolly, 1993), moubatin, has been isolated. Despite exhibiting a similar cysteine pattern, both ornithodorin and TAP display significant differences in amino acid sequence with the family of BPTI-like proteins (Figure 1). A series of mutational studies on TAP have called into question the role of the 'binding loop' and have implicated the N-terminal residues in TAP interaction with factor Xa (Dunwiddie *et al.*, 1992; Mao *et al.*, 1995).

TAP shows a BPTI-like solution structure as determined by NMR (Antuch *et al.*, 1994; Lim-Wilby *et al.*, 1995). Despite the availability of NMR structures of TAP and the crystal structure of factor Xa (Padmanabhan *et al.*, 1993), the determinants for the high affinity of TAP for factor Xa remain elusive. TAP has a 30-fold higher affinity for membrane-bound prothrombinase complex than for free factor Xa (Krishnaswamy *et al.*, 1994) and is an effective antithrombotic *in vivo* (Dunwiddie *et al.*, 1991; Schaffer *et al.*, 1991; Vlasuk *et al.*, 1991; Sitko *et al.*, 1992).

Results

Ornithodorin consists of two domains, residues 1′–53′ for the N-terminal and residues 61′–116′ for the C-terminal domains, linked by seven residues. Each of the two domains possesses the BPTI-like scaffold: one turn of a 3_{10} helix around the first cysteine residue, a double-stranded antiparallel β-sheet linked by a β-hairpin loop and a three turn α-helix (Figure 1). These secondary structure elements constitute the rounded bottom of a pear-shaped scaffold, which is lengthened by the binding loop and associated residues. The two domains are oriented tail-to-tail (Figure 2). It is particularly noteworthy that both 'reactive site loops' point away from the enzyme.

Structural comparison of the Kunitz domains

The lower part of these pear-shaped domains superimposes well with BPTI, reflected by the r.m.s. differences of the corresponding C_α atoms of 1.6 Å for 38 C_α atoms in the

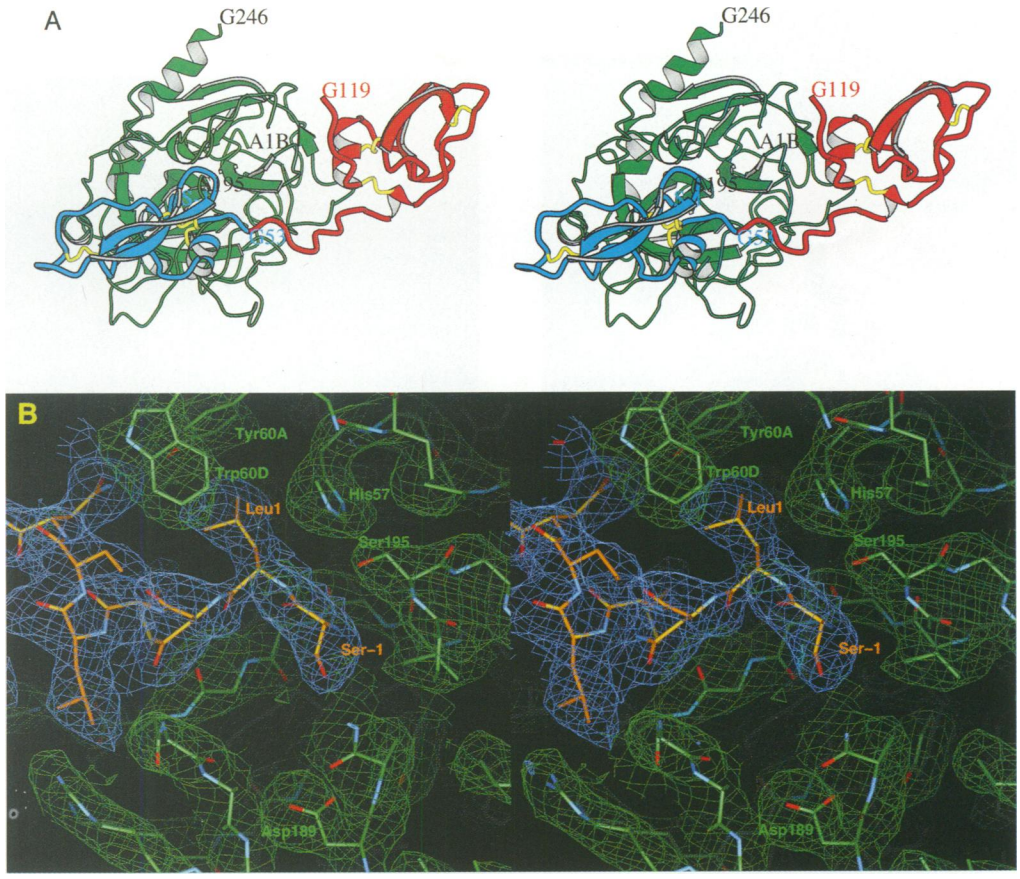

Fig. 2. The structure of the ornithodorin–thrombin complex. (**A**) Stereo view of the complex between ornithodorin (N-terminal domain cyan, C-terminal domain red) with thrombin (green). The view is into the active site cleft with the thrombin fibrinogen recognition exosite to the right. Yellow connections indicate disulfide bridges. The figure was generated with MOLSCRIPT (Kraulis, 1991). (**B**) Cyclic averaged electron density map around the N-terminus of ornithodorin contoured at 1.0 σ. The refined models of ornithodorin (orange) and thrombin (green) are superimposed. The view is from the right side of the complex, i.e. 90° rotated about *y* compared with (A). Figure prepared using MAIN (Turk, 1992).

N-terminal and 1.6 Å for 46 C_α atoms in the C-terminal domain with respect to BPTI. The better fit of the C-terminal domain is reflected throughout the domain, but again the best fit is seen at the base of the module. This structurally most conserved part of the BPTI scaffold encompasses a disulfide bridge (30I–51I), whose corresponding one disulfide intermediate is a well-populated state during the folding of BPTI and a direct precursor of the native structure (see Creighton, 1992).

A one-residue deletion in front of cysteines 13′ and 73′ respectively shifts their relative positions. The other disulfide bond partner is located in the inner loop of the Kunitz fold, which is four residues (one residue) shorter in the N-terminal (C-terminal) domain with respect to BPTI. This results in a significant displacement of the disulfide bridge, leading to major distortions in the binding loop conformation. These distortions are accompanied by sequence alterations which make the binding of this region to thrombin very unlikely, even in a canonical conformation. In particular, the residues at the putative P1 positions, Asn14′ and Ala74′, do not favour binding to thrombin. This is even more extreme for TAP, in which Asp16T formally corresponds to BPTI P1 residue Lys15I.

Ornithodorin interaction with thrombin

Neither of the two domains is therefore able to bind to serine proteinases according to the standard mechanism. Instead, it is the N-terminal residues from Ser–1′ (an additional N-terminal serine residue was introduced with the aim of recombinant expression) to Asn6′ of the first ornithodorin domain that contact the thrombin active site. The amino acids Ser–1′, Leu1′, Asn2′ and Val3′ run towards Ser195 and form a parallel β-sheet arrangement with thrombin segment Ser214–Gly219 (Figure 2). The free N-terminus of Ser–1′ is hydrogen bonded to O_γ of Ser195; in wild-type ornithodorin, the free N-terminus of Leu1′ could contribute the same interaction. The side chain of Ser–1′ points towards the specificity pocket, but does not penetrate it. The side chain of Leu1′ is accommodated in the hydrophobic pocket between Tyr60A and Trp60D (the thrombin S2 pocket), while Val3′ exhibits a hydrophobic interaction with Trp215 and Ile174. In turn, Trp60D is accommodated by a canyon formed between Leu1′, Asn6′ and Arg24′, the latter making a plane-to-plane stacking interaction with Trp60D. The environment of the carboxylate group of Glu192 is unfavourable, pointing towards the carbonyl groups of Ser–1′, Ala49′ and Cys50′. In the complex of wild-type ornithodorin with thrombin, this could be ameliorated via a stabilizing interaction of Glu192 with the free N-terminus of Leu1′.

Secondary contacts of the N-terminal domain are found between residues 24′–27′ (the β-hairpin loop) and the thrombin 60loop and between residues 40′, 45′, 48′ and 49′ of the α-helix with the thrombin 148loop. Altogether,

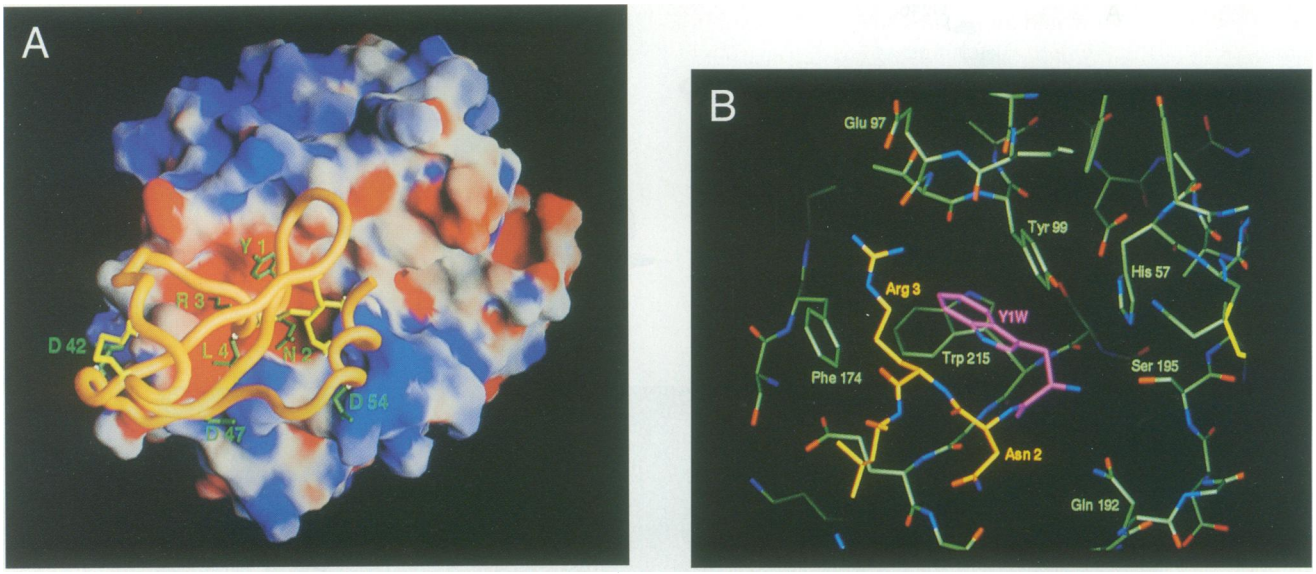

Fig. 3. Putative complex of factor Xa and TAP. (**A**) Model of the TAP–factor Xa complex. FactorXa is in the same orientation as thrombin in Figure 2A, with electrostatic potentials mapped onto its molecular surface. TAP is shown as a backbone worm and the side chains of those residues that upon mutation alter the inhibition constant by more than a factor of two are depicted as sticks. The complex has been modelled using the NMR structure of TAP (Antuch *et al.*, 1994; Lim-Wilby *et al.*, 1995), the crystal structure of factor Xa (Padmanabhan *et al.*, 1993) and the N-terminal residues of ornithodorin, on the assumption that TAP binds to factor Xa in a similar manner as the ornithodorin first domain to thrombin. Figure prepared using Grasp (Nicholls *et al.*, 1993). (**B**) Close-up view of the active site of factor Xa in its putative complex with the most potent TAP mutant Y1W(T). FactorXa is depicted in green and TAP residues are shown in orange. The mutated residue Trp1T is shown in pink. Figure prepared using MAIN (Turk, 1992).

two thirds of the van der Waals contacts and the hydrogen bonds between ornithodorin and thrombin are made by the N-terminal domain.

The region corresponding to Thr36′–Glu38′ is two residues longer in both BPTI and the C-terminal domain (Figure 1). In BPTI, the corresponding region would collide with the N-terminal residues, preventing them from contacting the active site. Furthermore, the β-hairpin loop is two residues longer in BPTI and one residue longer in TAP. As this segment constitutes the secondary binding region to the thrombin 60loop, neither BPTI nor TAP would fit the thrombin active site in this orientation. On the other hand, the shorter 60loop of factor Xa (Padmanabhan *et al.*, 1993) easily allows the accommodation of TAP.

The ornithodorin C-terminal domain shows less intimate contacts with thrombin, with interactions dominated by electrostatic forces. Three salt bridges (Glu60′–Arg67, Glu100′–Arg77A and Glu104′–Lys81) and the overall negative potential of this domain fix it to the thrombin fibrinogen recognition exosite. These contacts are strengthened by hydrophobic interactions between Phe103′, Val107′, Val111′, Ala112′ and Ile117′ and thrombin residues Phe34, Leu65, Tyr76, Met84 and the aliphatic part of the side chain of Lys36.

In all, 1800 Å^2 of the thrombin surface becomes buried on complex formation with ornithodorin, of which 1100 Å^2 is covered by the N-terminal domain alone. This is to be compared with the 800 Å^2 of the trypsin surface that is buried in the trypsin–BPTI complex (Huber *et al.*, 1974). It is perhaps noteworthy that roughly equivalent regions of the two ornithodorin domains are involved in contacts with thrombin (Figures 1 and 2), in particular the C-terminal α-helix.

Discussion

The interaction of the Kunitz inhibitor BPTI with trypsin (Huber *et al.*, 1974) has long been held as a paradigm for the interaction of serine proteinases with their inhibitors. The formation of a stable substrate-like interaction has also been observed for a wide range of 'small' inhibitors from varying sources and of varying scaffolds (Bode and Huber, 1992). The haematophage *O.moubata* provides the first example of a Kunitz-like serine proteinase inhibitor that does not obey the 'standard mechanism'. The alternative binding modes described here may have wider implications, not only for other serine proteinase inhibitors such as TAP, but also for Kunitz-like domains with no inhibitory properties.

Assuming that TAP binds to factor Xa in a similar manner to the N-terminal domain of ornithodorin to thrombin, we are able to explain the effects of almost all reported TAP mutants (Dunwiddie *et al.*, 1992; Mao *et al.*, 1995; Figure 3). In a TAP–factor Xa complex, Tyr1T points into the hydrophobic box lined by Tyr99, Phe174 and Trp215; this pocket could be better filled by the bulkier hydrophobic side chain of tryptophan in the mutant Y1W(T) (Figure 3), as noted for low molecular weight ligands of factor Xa (Stubbs *et al.*, 1995). This electronegative environment would be unfavourable for the mutant Y1E(T); furthermore, this mutant could form a salt bridge between Y1E(T) and Arg3T, interfering with the rearrangement of the N-terminus and thereby the interaction with factor Xa.

In agreement with acceptance of the additional N-terminal Ser–1′ in ornithodorin, an extension of the TAP N-terminus by a glycine residue does not alter the inhibitory potency. In contrast to the unfavourable interaction of thrombin Glu192 noted above, the equivalent

Gln192 in factor Xa would allow simultaneous favourable interactions with the free N-terminus and the carbonyl oxygens. In the ornithodorin–thrombin complex, the side chain of Asn2′ makes hydrogen bonds to both thrombin and the core structure of the ornithodorin N-terminal domain and may therefore direct correct folding of the N-terminus on proteinase binding, accounting for the conservation of Asn2′ in ornithodorin and TAP. Arg3T would fit into the prominent hydrophobic pocket of factor Xa shaped by Phe174 to accept hydrophobic side chain moieties, reaching towards the electronegative pocket described by the carbonyl groups of Ile175, Thr98 and Glu97 and the acidic side chain of the latter residue (Stubbs *et al.*, 1995). This structural feature may explain the beneficial effect of Arg3T and the dramatic consequences of its mutation. A positively charged Arg4T, as introduced by the mutation L4R(T), would collide with the positively charged S3 site formed by residues Arg222, Lys223 and Lys224 of factor Xa. TAP residues Asp47T and Asp54T point towards this basic patch in factor Xa, explaining the 3-fold decrease in affinity observed on replacing each by asparagine.

The conformation of the N-terminal residues of ornithodorin and their interaction with thrombin bear some similarity to hirudin and its thrombin complex (Grütter *et al.*, 1990; Rydel *et al.*, 1990): Leu1′ and Ile1 of hirudin occupy almost identical sites, as do Val3′ and hirudin Tyr3. Thr2 of hirudin is placed between Ser–1′ and Asn2′, but points in the same direction as Asn2′. Furthermore, the main chain conformation for the first three residues of hirudin is very similar to that of ornithodorin. As with hirudin (see Szyperski *et al.*, 1992), the N-terminal residues of TAP are disordered in solution (Antuch *et al.*, 1994); the necessary rearrangement of these residues on binding to factor Xa would explain the observed two step inhibition mechanism (Jordan *et al.*, 1992). The 'heretical' parallel β-sheet formation between an initially flexible N-terminal peptide and the target proteinase, as observed for hirudin, ornithodorin and TAP, is in stark contrast to the 'canonical' antiparallel β-sheet formation between a preformed binding loop and the cognate enzyme, exemplified by BPTI. That the two binding modes are observed for proteins of diverse origins but similar folds and functions raises interesting questions of molecular evolution.

It is striking that each of the macromolecular inhibitors of thrombin isolated from haematophages studied to date make use of the thrombin fibrinogen recognition exosite (Grütter *et al.*, 1990; Rydel *et al.*, 1990; van de Locht *et al.*, 1995). Not only does this make an important contribution to the affinity for thrombin, it also ensures that the inhibitor is not depleted by binding to other serine proteinases present in the blood. In contrast, TAP–factor Xa reveals no major exosite interaction. The fact that TAP is a far more potent inhibitor of prothrombinase than of free factor Xa (Krishnaswamy *et al.*, 1994) suggests that factor Va may provide additional exosite determinants for TAP binding.

In this paper, we have presented evidence for two novel binding modes of proteins bearing the Kunitz-type inhibitor fold, which may have more general implications for non-inhibitory members of this family. In β_2-bungarotoxin, the proposed ion channel binding region (Kwong *et al.*, 1995) is located roughly 30 Å from the antiprotease loop at the opposite end of the Kunitz module. This region corresponds to residues of the ornithodorin N-terminal domain that are in contact with thrombin and the proposed residues correspond to the secondary binding regions of ornithodorin to the thrombin 60loop and 148loop. Furthermore, the Kunitz domain of β_2-bungarotoxin is disulfide linked to the phospholipase moiety, so that the N-terminus of the Kunitz domain is free. Finally, the C-terminal helix of the β_2-bungarotoxin Kunitz domain has been shown to constitute the interface with phospholipase, reminiscent of the interaction of the ornithodorin C-terminal domain with thrombin (Figure 2).

Materials and methods

Bovine thrombin was prepared from ox blood (Brandstetter *et al.*, 1992). Recombinant ornithodorin, carrying an additional N-terminal serine residue (Ser–1′), was expressed in *Escherichia coli* (M.Otte, A.van de Locht, T.Friedrich, S.Bialojan, B.Kröger, C.Bollsch-Weiler, J.Dodt, E.A.Auerswald, W.Bode and H.Fritz, in preparation). Thrombin was co-crystallized with a slight excess of a 1:1 molar ratio of ornithodorin to thrombin. Monoclinic crystals (space group $P2_1$, containing four complexes per asymmetric unit) were grown at 20°C from 25% PEG 4000, 160 mM ammonium acetate, 80 mM sodium acetate, 200 mM ammonium sulfate, pH 5.0, in hanging drops using the vapour diffusion technique. Diffraction data up to 3.0 Å were collected on a MAR imaging plate system and evaluated using the Mosflm package (Leslie, 1994) and programs from the CCP4 Suite (CCP4, 1994).

The structure was solved using Patterson search techniques. Rotational and translational searches for the orientation and position of the thrombin molecules were performed with the program AMoRe (Navaza, 1994), using data up to 3.5 Å and the bovine thrombin model as previously obtained in complex with rhodniin (van de Locht *et al.*, 1995). The rotational search showed four solutions with correlation values of 6.4, 5.1, 4.8 and 4.0 σ. Translational search and rigid body fitting for these solutions resulted in a correlation value of 0.47, with the four independent molecules arranged as a pair of dimers. An initial envelope was created using the thrombin–rhodniin complex and the density was averaged using routines from the RAVE program package (Kleywegt and Jones, 1994). The envelope was improved progressively as the ornithodorin model could be fitted into the electron density. The averaged electron density allowed tracing of the complete ornithodorin chain. Several

Table I. Crystal data and refinement parameters for the ornithodorin–thrombin complex

Space group	$P2_1$
Cell constants (Å)	
a	125.3
b	89.9
c	101.4
β	108.4°
Limiting resolution (Å)	3.0
Significant measurements	94484
R_{merge}[a] (%)	14.1
Independent reflections	39528
Completeness	89.2% (∞–3.0 Å)
outermost shell	75.2% (3.13–3.0 Å)
Non-hydrogen protein atoms	12832
Solvent molecules	31
Reflections used for refinement	30140
Resolution range (Å)	10.0–3.1
Completeness (%)	80.4
R value[b] (%)	22.8
R.m.s. standard deviation	
bond lengths (Å)	0.012
bond angles (°)	1.60
RMSB[c] (Å^2)	1.54

[a]$R_{merge} = \Sigma(I-\langle I\rangle)/\Sigma I$.
[b]R value $= \Sigma(|F_{obs}|-|F_{calc}|)/\Sigma|F_{obs}|$.
[c]RMSB, r.m.s. deviation of the B factor of bonded atoms.

refinement cycles, consisting of model building using FRODO (Jones, 1978) and O (Jones *et al.*, 1991) and conjugate gradient minimization with X-PLOR (Brünger, 1992) using the parameters of Engh and Huber (1991), reduced the *R* value to 0.23. Thirty one of the conserved water molecules from serine proteases (Sreenivasan and Axelsen, 1992) were added to the model. Data statistics are given in Table I. The coordinates of the ornithodorin–thrombin complex have been deposited with the Brookhaven Protein Databank.

Acknowledgements

We thank H.Brandstetter, R.Engh and D.Turk for stimulating and fruitful discussion and M.Schneider for preparation of the figures. This work was supported by the Sonderforschungsbereich 207 and EU contract BMH4-CT96-D937.

References

Antuch,W., Berndt,K.D., Chávez,M.A., Delfín,J. and Wüthrich,K. (1993) The NMR solution structure of a Kunitz-type proteinase inhibitor from the sea anemone *Stichodactyla helianthus*. *Eur. J. Biochem.*, **212**, 675–684.

Antuch,W., Güntert,P., Billeter,M., Hawthorne,T., Grossenbacher,H. and Wüthrich,K. (1994) NMR solution structure of the recombinant tick anticoagulant protein (rTAP), a factor Xa inhibitor from the tick *Ornithodoros moubata*. *FEBS Lett.*, **352**, 251–257.

Ascenzi,P., Coletta,M., Amiconi,G., de Cristofaro,R., Bolognesi,M., Guarneri,M. and Menegati,E. (1988) Binding of the bovine basic pancreatic trypsin inhibitor (Kunitz) to human α-, β- and γ-thrombin; a kinetic and thermodynamic study. *Biochim. Biophys. Acta*, **956**, 156–161.

Barton,G.J. (1993) ALSCRIPT a tool to format multiple sequence alignments. *Protein Engng*, **1**, 37–40.

Bode,W. and Huber,R. (1992) Natural protein proteinase inhibitors and their interaction with proteinases. *Eur. J. Biochem.*, **204**, 433–451.

Bode,W., Mayr,I., Baumann,U., Huber,R., Stone,S.R. and Hofsteenge,J. (1989) The refined 1.9 Å crystal structure of human α-thrombin: interaction with D-Phe–Pro–Arg chloromethylketone and significance of the Tyr–Pro–Pro–Trp insertion segment. *EMBO J.*, **8**, 3467–3475.

Bode,W., Turk,D. and Karshikov,A. (1992) The refined 1.9 Å X-ray crystal structure of D-PheProArg chloromethylketone inhibited human α-thrombin. Structure analysis, overall structure, electrostatic properties, detailed active site geometry, structure–function relationships. *Protein Sci.*, **1**, 426–471.

Brandstetter,H., Turk,D., Höffken,H.W., Grosse,D., Stürzebecher,J., Martin,P.D., Edwards,B.F.P. and Bode,W. (1992) Refined 2.3 Å X-ray crystal structure of bovine thrombin complexes formed with the benzamidine and arginine-based thrombin inhibitors NAPAP, 4-TAPAP and MQPA. *J. Mol. Biol.*, **226**, 1085–1099.

Brünger,A.T. (1992) *X-PLOR, Version 3.1. A System for X-ray Crystallography and NMR*. Yale University Press, New Haven, CT.

CCP4 (1994) The CCP4 Suite: Collaborative Computational Project, Number 4. *Acta Crystallogr.*, **D50**, 760–763.

Creighton,T.E. (1992) The disulphide folding pathway of BPTI. *Science*, **256**, 111–112.

Deisenhofer,J. and Steigemann,W. (1975) Crystallographic refinement of the structure of bovine pancreatic trypsin inhibitor at 1.5 Å resolution. *Acta Crystallogr.*, **B31**, 238–250.

Dunwiddie,C.T., Smith,D.E., Nutt,E.M. and Vlasuk,G.P. (1991) Anticoagulant effects of the selective factor Xa inhibitors tick anticoagulant peptide and antistasin in the APTT assay are determined by the relative rate of prothrombinase inhibition. *Thromb. Res.*, **64**, 787–794.

Dunwiddie,C.T., Neeper,M.P., Nutt,E.M., Waxman,L., Smith,D.E., Hofmann,K.J., Lumma,P.K., Garsky,V.M. and Vlasuk,G.P. (1992) Site-directed analysis of the functional domains in the factor Xa inhibitor tick anticoagulant peptide: identification of two distinct regions that constitute the enzyme recognition sites. *Biochemistry*, **31**, 12126–12131.

Engh,R.A. and Huber,R. (1991) Accurate bond and angle parameters for X-ray protein structure refinement. *Acta Crystallogr.*, **A47**, 392–400.

Grütter,M.G., Priestle,J.P., Rahuel,J., Grossenbacher,H., Bode,W., Hofsteenge,J. and Stone,S.R. (1990) Crystal structure of the thrombin–hirudin complex: a novel mode of serine protease inhibition. *EMBO J.*, **9**, 2361–2365.

Huber,R., Kukla,D., Rühlmann,A., Epp,O. and Formanek,H. (1970) The basic trypsin inhibitor of bovine pancreas. *Naturwissenschaften*, **57**, 389–392.

Huber,R., Kukla,D., Bode,W., Schwager,P., Bartels,K., Deisenhofer,J. and Steigemann,W. (1974) Structure of the complex formed by bovine trypsin and bovine pancreatic trypsin inhibitor. II. Crystallographic refinement at 1.9 Å resolution. *J. Mol. Biol.*, **89**, 73–101.

Jones,T.A. (1978) A graphics model building and refinement system for macromolecules. *J. Appl. Crystallogr.*, **11**, 268–272.

Jones,T.A., Zou,J.-Y., Cowan,S.W. and Kjeldgaard,M. (1991) Improved methods for building protein models in electron density maps and location of errors in these models. *Acta Crystallogr.*, **A47**, 110–119

Jordan,S.P.,Mao,S.-S., Lewis,S.D. and Shafer,J.A. (1992) Reaction pathway for inhibition of blood coagulation factor Xa by tick anticoagulant peptide. *Biochemistry*, **31**, 5374–5380.

Kleywegt,G.J. and Jones,T.A. (1994) Halloween...masks and bones. In *From First Map to Final Model*. CCP4, Danesbury Laboratory, UK, pp. 59–66.

Kraulis,P.J. (1991) MOLSCRIPT: a program to produce both detailed and schematic plots of proteins. *J. Appl. Crystallogr.*, **24**, 946–950.

Krishnaswamy,S., Vlasuk,G.P. and Bergum,P.W. (1994) Assembly of the prothrombinase complex enhances the inhibition of bovine factor Xa by tick anticoagulant peptide. *Biochemistry*, **33**, 7897–7908.

Kwong,P.D., McDonald,N.Q., Sigler,P. and Hendrickson,W.A. (1995) Structure of β_2-bungarotoxin:potassium channel binding by Kunitz modules and targeted phospholipase action. *Structure*, **3**, 1109–1119.

Lancelin,J.-M., Foray,M.-F., Poncin,M., Hollecker,M., and Marion,D. (1994) Proteinase inhibitor homologues as potassium channel blockers. *Nature Struct. Biol.*, **1**, 246–250.

Laskowski,M. and Kato,I. (1980) Protein inhibitors of proteinases. *Annu. Rev. Biochem.*, **49**, 593–626.

Leslie,A.G.W. (1994) *Mosflm User Guide, Mosflm Version 5.20*. MRC Laboratory of Molecular Biology, Cambridge, UK.

Lim-Wilby,M.S.L., Hallenga,K., de Maeyer,M., Lasters,I., Vlasuk,G.P. and Brunck,T.K. (1995) NMR structure determination of tick anticoagulant peptide (TAP). *Protein Sci.*, **4**, 178–186.

Lottenberg,R., Hall,J.A., Blinder,M., Binder,E.P. and Jackson,C.M. (1983) The action of thrombin on peptide *p*-nitroanilide substrates. Substrate selectivity and examination of hydrolysis under different reaction conditions. *Biochim. Biophys. Acta*, **742**, 539–557.

Mao,S.-S., Huang,J., Welebob,C., Neeper,M.P., Garsky,V.M. and Shafer,J.A. (1995) Identification and characterization of variants of tick anticoagulant peptide with increased inhibitory potency toward human factor Xa. *Biochemistry*, **34**, 5098–5103.

Markwardt,F. (1994) Coagulation inhibitors from blood-sucking animals. *Pharmazie*, **49**, 313–316.

Navaza,J. (1994) AMoRe: an automated package for molecular replacement. *Acta Crystallogr.*, **A50**, 157–163.

Nicholls,A., Bharadwaj,R. and Honig,B. (1993) Grasp—graphical representation and analysis of surface properties. *Biophys. J.*, **64**, A166.

Padmanabhan,K., Padmanabhan,K.P., Tulinsky,A., Park,C.H., Bode,W., Huber,R. and Kisiel,W. (1993) Structure of human des(1–45) factor Xa at 2.2 Å resolution. *J. Mol. Biol.*, **232**, 947–966.

Rydel,T.J., Ravichandran,K.G., Tulinsky,A., Bode.W., Huber,R., Roitsch,C. and Fenton,J.W. (1990) The structure of a complex of recombinant hirudin and human α-thrombin. *Science*, **249**, 277–280.

Schaffer,L.W., Davidson,J.T., Vlasuk,G.P. and Siegl,P.K.S. (1991) Antithrombotic efficacy of recombinant tick anticoagulant peptide. *Circulation*, **84**, 1741–1748.

Sitko,G.R., Ramjit,D.R., Stabilito,H., Lehman,D., Lynch,J.J. and Vlasuk,G.P. (1992) Conjunctive enhancement of enzymatic thrombolysis and prevention of thrombotic reocclusion with the selective factor Xa inhibitor, tick anticoagulant peptide. *Circulation*, **85**, 805–814.

Sreenivasan,U. and Axelsen,P.H. (1992) Buried water in homologous serine proteases. *Biochemistry*, **31**, 12785–12791.

Stubbs,M.T. and Bode,W. (1993) A player of many parts: the spotlight falls on the thrombin structure. *Thromb. Res.*, **69**, 1–58.

Stubbs,M.T. and Bode,W. (1995) The clot thickens: clues provided by thrombin structure. *Trends Biochem. Sci.*, **20**, 23–28.

Stubbs,M.T., Huber,R. and Bode,W. (1995) Crystal structures of factor Xa specific inhibitors in complex with trypsin: structural grounds for inhibition of factor Xa and selectivity against thrombin. *FEBS Lett.*, **375**, 103–107.

Szyperski,T., Güntert,P., Stone,S.R., Tulinsky,A., Bode,W., Huber,R. and Wüthrich,K. (1992) Impact of protein–protein contacts on the conformation of thrombin-bound hirudin studied by comparison with

the nuclear magnetic resonance solution structure of hirudin(1–51). *J. Mol. Biol.*, **228**, 1206–1211.

Turk,D. (1992) Weiterentwicklung eines Programms für Molekülgraphik und Elektronendichte-Manipulation und seine Anwendung auf verschiedene Protein-Strukturaufklärungen. Ph.D. thesis. Technische Universität München, Munich, Germany.

van de Locht,A., Lamba,D., Bauer,M., Huber,R., Friedrich,T., Kröger,B., Höffken,W. and Bode,W. (1995) Two heads are better than one: crystal structure of the insect derived double domain Kazal inhibitor rhodniin in complex with thrombin. *EMBO J.*, **14**, 5149–5157.

Vlasuk,G.P. (1993) Structural and functional characterization of tick anticoagulant peptide (TAP): a potent and selective inhibitor of blood coagulation factor Xa. *Thromb. Haemostasis*, **70**, 212–216.

Vlasuk,G.P., Ramjit,D., Fujita,T., Dunwiddie,C.T., Nutt,E.M., Smith,D.E. and Shebuski,R.J. (1991) Comparison of the *in vivo* anticoagulant properties of standard heparin and the highly selective factor Xa inhibitors antistasin and tick anticoagulant peptide (TAP) in a rabbit model of venous thrombosis. *Thromb. Haemostasis*, **65**, 257–262.

Waxman,L. and Connolly,T.M. (1993) Isolation of an inhibitor selective for collagen-stimulated platelet aggregation from the soft tick *Ornithodoros moubata*. *J. Biol. Chem.*, **268**, 5445–5449

Waxman,L., Smith,D.E., Arcuri,K.E. and Vlasuk,G.P. (1990) Tick anticoagulant peptide (TAP) is a novel inhibitor of blood coagulation factor Xa. *Science*, **248**, 593–596.

Received on July 1, 1996; revised on July 23, 1996